

# Experimental and computational study of Trachyspermum leaves extract as a green inhibitor for corrosion inhibition of mild steel in HCl

**Niloofar Jafari**

Islamic Azad University

**Sayed Ali Ahmadi** (✉ [ahmadi.iauk58@gmail.com](mailto:ahmadi.iauk58@gmail.com))

Islamic Azad University

**Razieh Razavi**

University of Jiroft

---

## Research Article

**Keywords:** Trachyspermum, Corrosion, Mild steel, Hydrochloric acid, Adsorption, Langmuir isotherm

**Posted Date:** July 12th, 2022

**DOI:** <https://doi.org/10.21203/rs.3.rs-917730/v2>

**License:**  This work is licensed under a Creative Commons Attribution 4.0 International License.

[Read Full License](#)

---

# **Experimental and computational study of Trachyspermum leaves extract as a green inhibitor for corrosion inhibition of mild steel in HCl**

**Niloofar Jafari<sup>1</sup>, Sayed Ali Ahmadi<sup>1,\*</sup>, Razieh Razavi<sup>2</sup>**

<sup>1</sup>Department of Chemistry, Kerman Branch, Islamic Azad University, Kerman, Iran.

<sup>2</sup>Department of Chemistry, Faculty of Science, University of Jiroft, Jiroft, Iran

\*Corresponding author E-mail: [sahmadi@iauk.ac.ir](mailto:sahmadi@iauk.ac.ir), [ahmadi.iauk58@gmail.com](mailto:ahmadi.iauk58@gmail.com)

## **ABSTRACT**

The present study aims at investigating the impacts of the extract of Trachyspermum leaves on the mild steel corrosion in 0.1M hydrochloric acid (HCl), while highlighting its inhibitory mechanisms. The effects of mild steel corrosion in solutions of HCl were examined using the gravimetric and galvanostatic polarization techniques, along with EIS analyses. According to the EIS data, the highest coating undamaged index (83 %) after 100 h of immersion. According to the results, the maximum inhibitory effectiveness corresponding to the minimum corrosion rate could be observed at the highest desirable level of inhibitor concentration equal to 100 ppm, while the corrosion rate decreases with an increase in the extract concentration. The absorption examinations indicated the best description of the metal surface interaction by Langmuir isotherm with  $-31.85\text{KJmol}^{-1}$ , while obtaining the best exposure time for the Trachyspermum leaves extract adsorption into the surface of the metal in different concentrations. SEM, AFM, IR, and XRD showed the good coverage of Trachyspermum on the surface of mild steel. Based on the results of polarization, the inhibitors can play the role of a mixed inhibitor, also confirmed by the computational data.

**Keywords:** Trachyspermum, Corrosion, Mild steel, Hydrochloric acid, Adsorption, Langmuir isotherm

## **1. Introduction**

One of the significant problems faced by different industries is the mild steel corrosion<sup>1-3</sup> in acids, particularly hydrochloric acid. Moderation of such adverse phenomena through the application of organic materials is essential to inhibit corrosion. The collective work of different scholars has focused on developing efficient inhibitors to secure metallic materials against corrosion<sup>4-6</sup>. Research has shown that the direct, as well as indirect costs of corrosion processes, make up around 3-4% of the gross domestic product of developed nations each year<sup>5,7</sup>. Several major industrial processes, including steel pickling, oil wells acidification, ion exchanger regeneration, processing of leather, producing organic as well as inorganic compounds, and industrial cleansing use Hydrochloric acid (HCl) solution<sup>7-9</sup>.

Application of acid inhibitors in different industrial procedures is typically aimed at controlling metal corrosion<sup>10-13</sup>, making their application considerable convenient in protecting against corrosion<sup>5, 14-18</sup>. Hence, undesirable metal dissolution and acid consumption can be prevented, especially when an acid solution is used<sup>19</sup>. Many acid inhibitors belong to organic molecules, which contain oxygen, nitrogen, or sulfur atoms in a conjugated system, playing an efficient role as corrosion inhibitors. Different inhibitors that contain N have been studied by scholars concerning the corrosion inhibitory features for metals in acid media<sup>20</sup>. Organic inhibitors that contain N atom act strongly for metals in acid solutions<sup>5, 21-25</sup>. Different studies have investigated the effects of plant extracts as green inhibitors for corrosion because they do not pollute the environment and are eco-friendly, inexpensive, and easy to access from nature. Research shows that products taken from nature<sup>26</sup> and coming from plants have different organic substances<sup>5,16-18</sup> such as alkaloids<sup>27</sup>, tannins<sup>28</sup>, pigments<sup>29</sup>, organic<sup>30,31</sup> and amino acids<sup>5, 32</sup>, making them popular for their inhibitory effects<sup>5, 21, 33-38</sup>. This study aims at providing the Trachyspermum<sup>39-48</sup> extract

and investigating its corrosion resistance as a corrosion inhibitor for mild steel using a solution of 0.1M HCl according to gravimetric assessments, electrochemical impedance spectroscopy, and potentiodynamic polarization assessments. It also studies the influence of the inhibitors' structural parameters on the effectiveness of the inhibition as well as the adsorption mechanisms on the surface of metal while correlating the experimental data with quantum chemical parameters.

## **2. Experimental**

### **2-1. Preparation of the working electrode**

A nominal (wt%) composition of Fe =97.84%, Mn =1.4%, P=0.045%, C =0.17%, N=0.009 % and Si=0.5%. was considered for the mild steel rod (a diameter of 1 cm) in the present work. Soldering the same steel samples to coated Cu-wires for electrical connections with a 1 cm<sup>2</sup> laid open zone aimed at conducting electrochemical investigations. Mechanical abrasion of the working electrode surface was performed using various grades of papers, 600, 800, 1000, and 1500 before measurement. Then, distilled water was used along with acetone to rinse the samples of mild steel, after which drying was done using warm airflow.

### **2-2. preparation of inhibitor and electrolytes**

Distilled water was used to clean Trachyspermum leaves from fiery residues of mud. Leaf drying over a 48-74-hour period in the thermostat with a temperature of 60 °C, grinding, and obtaining the leaf powder were the next steps, followed by refluxing and shacking 100 mg of the Trachyspermum powder with a mixture of ethanol and water at a temperature of 75 °C over 24 hours. After filtering the refluxed product, evaporation of the obtained solution was performed to 100 ml of dark brown reside followed by drying in a vacuum drying oven using a temperature of

60 °C during 48 hours. Procurement of the light brown deposit (about 2.5g material) and its saving in a vacuum desiccator were the next steps. Dilution of the hydrochloric acid to 0.1M HCl aimed at preparing the corrosion medium. Dilution of the extract with 0.1M HCl was carried out to obtain various concentrations of *Trachyspermum* leaves extract (30, 45, 70, 100 mg/L). The reagent grade, 37% HCl (Sigma Aldrich), as well as distilled water, were used to prepare the corrosion solution (0.1M HCl). Different concentrations (30, 45, 70, 100 mg/L) were considered to prepare the inhibitor solution, leading to the highest *Trachyspermum* extract solvency in 0.1M HCl up to 500 mg/L.

### **2-3. Plant material**

Leaves of *Trachyspermum* (*Trachyspermum ammi*) were purchased from the traditional herbal market, Tehran, Iran in June, 2020. A voucher specimen has been deposited at the Herbarium of the Department of Pharmacognosy, Faculty of Pharmacy, Tehran University of Medical Sciences, Tehran, Iran (PMP-657).

### **2-4 . Gravimetric measurements**

Calculations of the mild steel samples were set up according to ASTM G 31–72 to perform gravimetric assessments<sup>49</sup> over, for 24 hours at 298 K. After preparation of 0.1M HCl acid blank solution which contained 30, 45, 70, 100 mg/L of the extract of *Trachyspermum* leaves, soaking of the pre-weighted metal samples in the prepared solution was carried out. Exclusion of the metal samples, deliberate rinsing with acetone, drying with nitrogen flow, and weighing to electronic balance were all performed after drenching. The experimental temperature remained stable. Three replications have been presented in the present work.

### **2-5 . Electrochemical measurements**

Electrochemical assessments were performed using Estate Electrochemical Workstation. The cell system has three electrodes, including the mild steel, platinum, and saturated calomel electrodes (SCE) in the form of working, counter, and reference electrodes, correspondingly. A working area of 1 cm<sup>2</sup> was considered for the samples to perform electrochemical assessments. A stable open circuit potential (OCP) was initially obtained by soaking the working electrode into the test solution. The frequencies of 100 kHz to 0.01 Hz were considered to scan the electrochemical impedance spectroscopy (EIS) considering a signal amplitude perturbation of 5 mV at OCP. Considering OCP at 1 mV/s scan rate, a scan of  $\pm$  250 mV against SCE was used to record the potentiodynamic polarization curves. Three replications of the electrochemical assessments resulted in reliable values.

## **2-6. Quantum chemical studies**

Quantum chemical estimations were performed using the density functional theory (DFT) at a B3LYP function considering 6–311G+ (d, p) basis set for molecules with Gaussian 03 project programming to examine the effects of inhibitor molecular structure as well as electronic features on the effectiveness of inhibition. The optimized structures in the gas phase were considered to obtain the main parameters such as the lowest unoccupied molecular orbital (ELUMO) energy, the highest occupied molecular orbital (EHOMO), energy gap ( $\Delta E$ ) of the LUMO and HOMO, total energy (T.E.), electronegativity ( $\chi$ ), molecules softness ( $\sigma$ ) as well as hardness ( $\eta$ ), the energy distinction of the molecule electron exchange and dipole moment ( $\mu$ ), chemical potential ( $\pi$ ), the number of transferring electrons ( $\Delta N$ ), etc. the use of the gas phase to perform theoretical estimations is supposed to be a suitable strategy as there are no significant differences with the results of the aqueous phase, while there is a significant decrease in the estimation time<sup>50</sup>.

## **2-7. Surface morphology studies (SEM analysis)**

The scanning electron microscope was used to observe the samples' surface morphology following the immersion of the pre-heated samples in 0.1M HCl solution in the absence and presence of 500 mg/L Trachyspermum leaves extract over a 24-hour period at 298 K. Doubled distilled water and acetone were used to rinse the surface of the samples, followed by drying to obtain the necessary information on the surface morphology of the samples.

## **3. Results and discussion**

### **3-1. Potentiodynamic polarization measurements**

Polarization tests were recorded and some electrochemical parameters were attained from the polarization curves containing corrosion current density ( $i_{corr}$ ), corrosion potential ( $E_{corr}$ ), anodic and cathodic Tafel slopes ( $\beta_a, \beta_c$ ), and inhibition efficiency (IE, labeled also as  $\eta$ ). The IE was calculated using the following equation:

$$\eta(\%) = \frac{i_{corr} - i_{corr}^{inh}}{i_{corr}} \times 100$$

in which  $i_{corr}$  and  $i_{corr}^{inh}$  represent the current densities of corrosion in blank solution and 0.1M HCl consisting of inhibitor, correspondingly. Figure 1 indicates the steel polarization plots, taken five minutes following immersion in blank solution and 0.1M HCl consisting of inhibitor. Figure 2 showed the OCP diagram of electrode. Table 1 shows the obtained electrochemical data, according to which the greatest IE for both inhibitors can be observed at the maximum concentration of 100 mg/L after 5 minutes immersion.

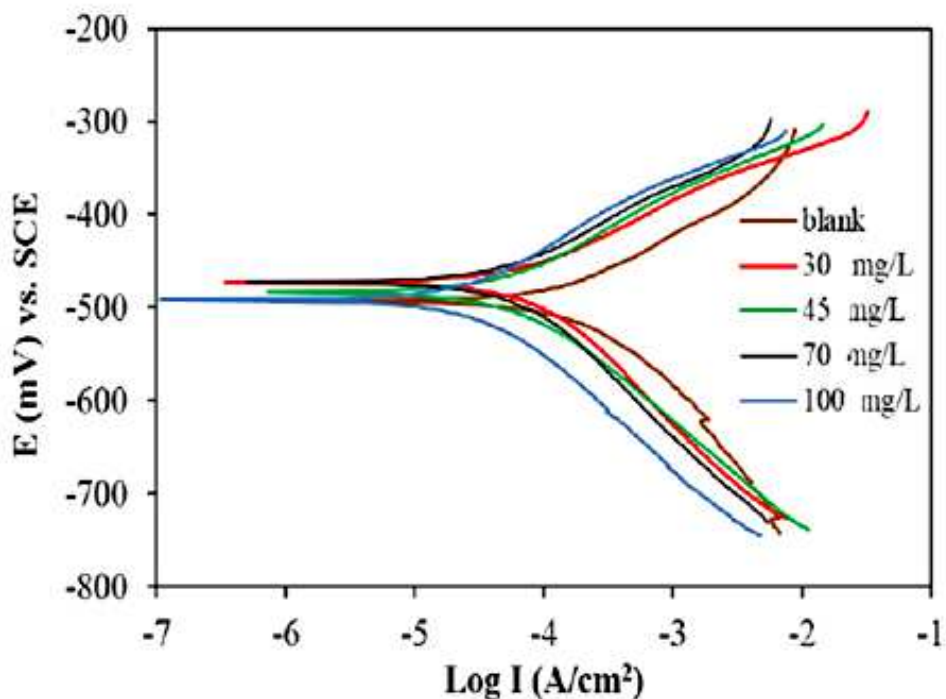


**Figure 1.** Tafel curves for steel in 0.1M HCl solutions in the absence and presence of different Trachyspermum concentrations following immersion for five minutes.

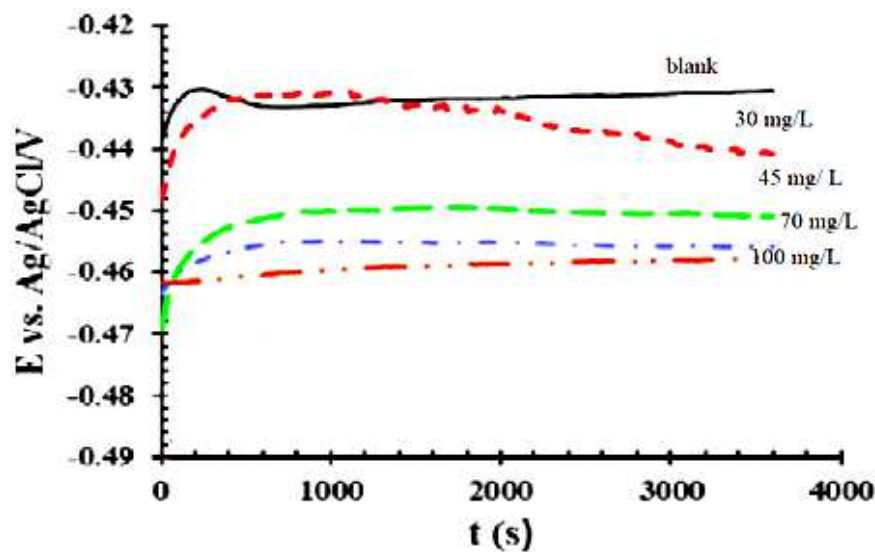


**Figure 2.** OCP of working electrode in 0.1M HCl solutions in the absence and presence of different Trachyspermum concentrations

**Table 1.** Obtained electrochemical data using Tafel curves for steel in 0.1M HCl considering various Trachyspermum concentrations.

| C(mg/L) | E(mV) | $i_{corr}$ ( $\mu\text{A}/\text{cm}^2$ ) | $\beta_a$ (mV/dec) | $\beta_c$ (mV/dec) | %IE   |
|---------|-------|------------------------------------------|--------------------|--------------------|-------|
| 0       | -425  | 710                                      | 99                 | 462                | -     |
| 30      | -459  | 339                                      | 56                 | 310                | 89.20 |
| 45      | -477  | 320                                      | 50                 | 109                | 90.1  |
| 75      | -483  | 312                                      | 43                 | 214                | 96.35 |
| 100     | -490  | 290                                      | 40                 | 243                | 98.20 |

When the shift in the  $E_{corr}$  is  $<85$  mV due to the inhibitor presence, the inhibitor will belong to the mixed type<sup>51, 52</sup>, while it will be cathodic or anodic based on the shift direction in other conditions. As the  $E_{corr}$  shift was  $<85$  mV in this research, the molecule belonged to the mixed type. Nevertheless, as shown in Figure 1, Trachyspermum functions as a mixed type when it is immersed for five minutes. Meantime, Trachyspermum affected cathodic and anodic reactions significantly. According to Table 1, fewer values of  $i_{corr}$  of Trachyspermum are observed as inhibition concentration, indicating that Trachyspermum has highly active inhibition characteristics.

### 3-2. Electrochemical impedance spectroscopy

The Nyquist plots and Bode plots associated with the mild steel in 0.1M HCl solutions are shown in Figures 3 and 4 in the absence and presence of different inhibitor concentrations following immersion for five minutes. Fitting of the EIS results with the equivalent circuit was performed according to Figure 5, in which  $R_s$ ,  $R_{ct}$ , and CPE indicate solution resistance, charge transfer resistance, and the constant phase element, correspondingly. Figure 3 indicates an increase in the semicircle diameter based on the inhibitor concentration. Table 2 indicates Impedance data collected through the test, in which the equation below was used to calculate the IE ( $\eta$ ):

$$\eta(\%) = \frac{R_{ct}^{inh} - R_{ct}}{R_{ct}^{inh}} \times 100$$

In which  $R_{ct}^{inh}$  and  $R_{ct}$  reflect the charge transfer resistance in the inhibited as well as uninhibited system, correspondingly.

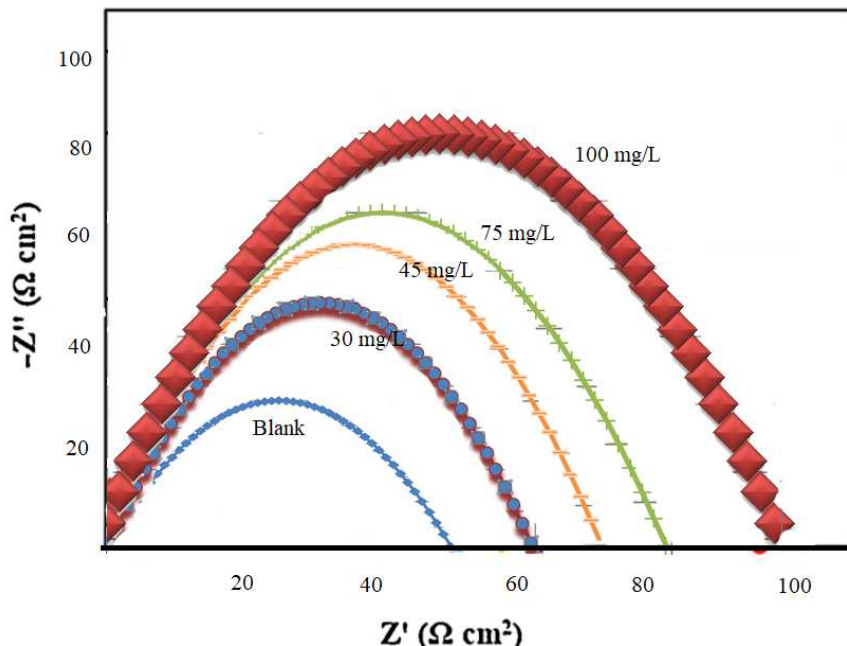


**Figure 3.** Nyquist plots obtained for mild steel in 0.1M HCl solution in the absence and presence of different Trachyspermum concentrations

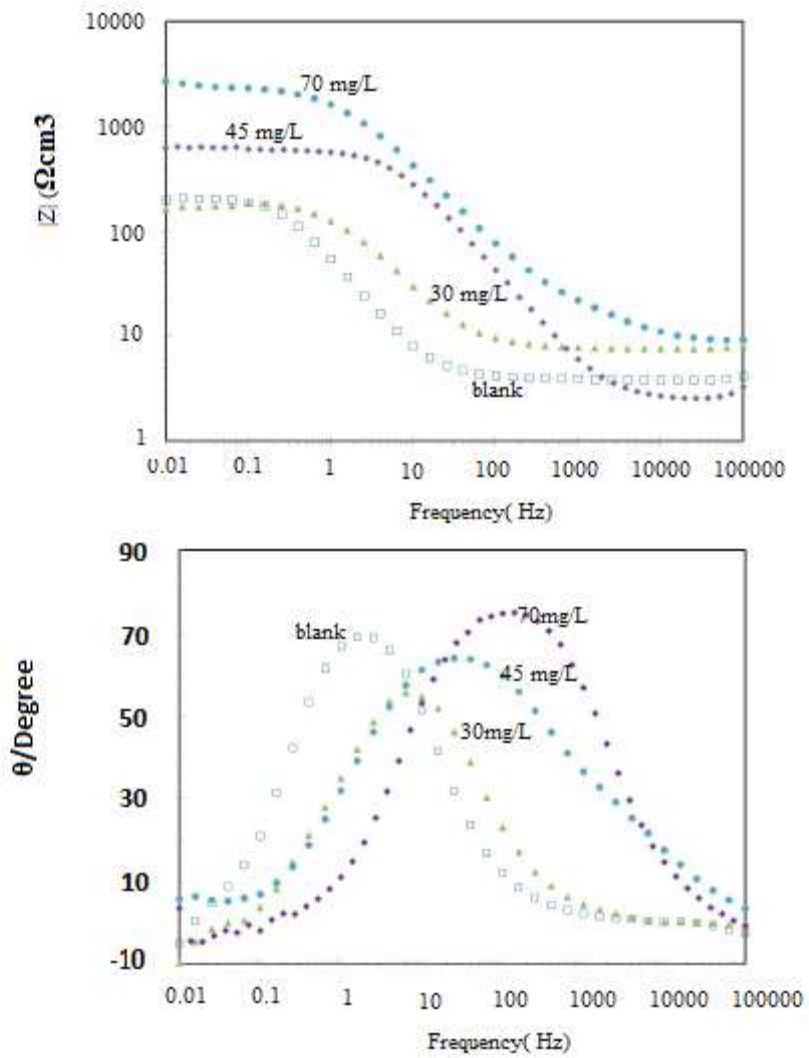


**Figure 4.** Bode plots of the for mild steel in 0.1M HCl solution in the absence and presence of different Trachyspermum concentrations

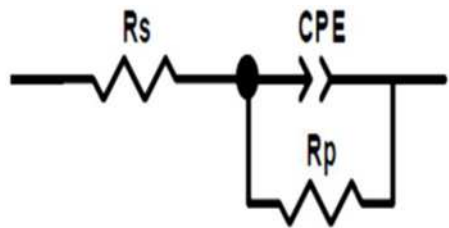


**Figure 5.** Electrical equivalent circuit illustration was employed for the analysis of results.

**Table 2.** Impedance data was collected using EIS tests for steel in blank solution and 0.1M HCl considering various concentrations of inhibitors following 5 minutes.

| C(mg/L) | R <sub>ct</sub> (Ω.cm <sup>2</sup> ) | CPE(μFcm <sup>-2</sup> ) | n     | η%   |
|---------|--------------------------------------|--------------------------|-------|------|
| Blank   | 242                                  | 94.5                     | 0.842 | -    |
| 30      | 785                                  | 76.2                     | 0.854 | 71   |
| 45      | 940                                  | 62.1                     | 0.868 | 75   |
| 70      | 1075                                 | 49.01                    | 0.875 | 78.5 |
| 100     | 1248                                 | 44.0                     | 0.892 | 83   |

According to Table 2, the  $R_{ct}$  values face an increasing trend based on the inhibitor concentration after immersing for five minutes. However, there is a general reduction in the CPE values, reflecting an increasing trend in corrosion inhibition. The decrease in CPE is associated with the increase of the thickness of the protective layer or the reduction of the local dielectric constant ( $D$ )<sup>53</sup>. The findings show similarities between the results obtained by EIS investigations and polarization assessments. The results showed higher values for Trachyspermum corrosion inhibitory effects with the greatest value at 100 mg/L. The capacitance values of the double-layer were calculated by EIS data  $124.8 \times 10^{-5} \mu\text{F}/\text{cm}^2$  for concentration 100mg/L. For comparing inhibition effect Table 3 obtained important data.

**Table 3.** comparative inhibition effect of several green inhibitors

| Green inhibitor                              | $\eta$ % |
|----------------------------------------------|----------|
| This study (100 mg/L)                        | 80 %     |
| Camphor <sup>3</sup> (600 mg/L)              | 89 %     |
| Magnolia grandiflora <sup>7</sup> (500 mg/L) | 85 %     |
| Primrose flower <sup>6</sup> (700 mg/L)      | 80 %     |

### **3-3. Surface morphology**

The SEM images of the currently polished steel specimens and those soaked in 0.1M HCl are displayed in Figure 6 in conditions that inhibitor (100 mg/L Trachyspermum) has been absent and present following two hours. Obviously, the damage and pits occur when the inhibitor is absent, but there is a significant reduction in the damage and pits resulting from corrosion when 100mg/L inhibitor is present. A protective layer is created on the steel by the inhibitor, which preserves the steel against the corrosive attacks that lead to fewer black pits. Besides, as shown in Figure 6, when Trachyspermum is present, there are no black pits or holes, reflecting that Trachyspermum has better corrosion inhibitory effects. The findings are completely in line with the data collected through electrochemical assessments.

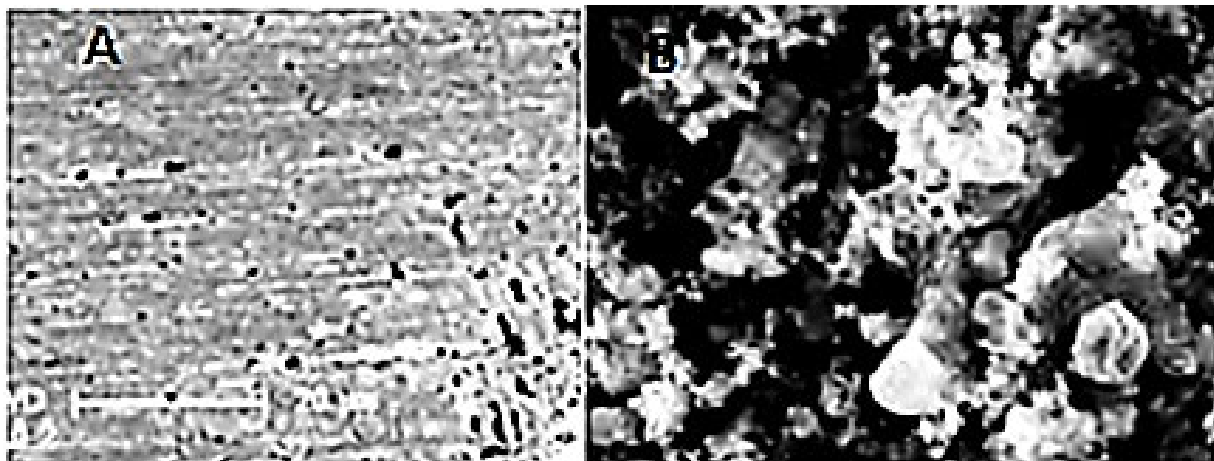


**Figure 6.** SEM images for (A) steel samples two hours following immersion in blank solution 0.1M HCl; (B) steel samples two hours following immersion in 100mg/L of Trachyspermum.

By XRD pattern and IR spectrum, and AFm analysis the surface changing after using Trachyspermum. As an inhibitor, the coverage of the surface by Trachyspermum can be found exactly (Figures 7-9). By IR spectrum the recognition of the presence of the organic compound in the surface of mild steel after adding the 100 mg/L of Trachyspermum can be confirmed. The big peak in  $3400\text{ cm}^{-1}$  can refer to the organic group of compounds.

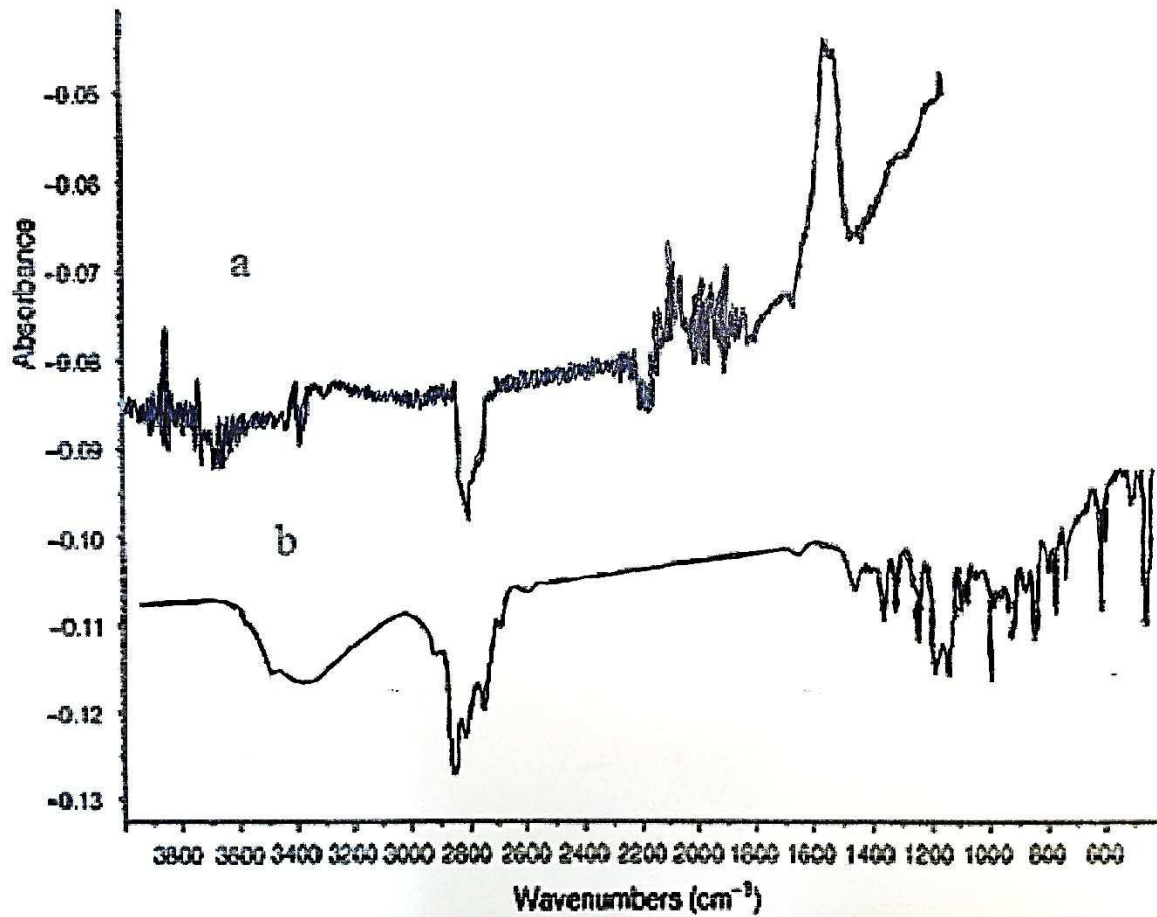


**Figure 7.** IR spectrum for (A) steel samples two hours following immersion in blank solution 0.1M HCl; (B) steel samples two hours following immersion in 100mg/L of Trachyspermum.

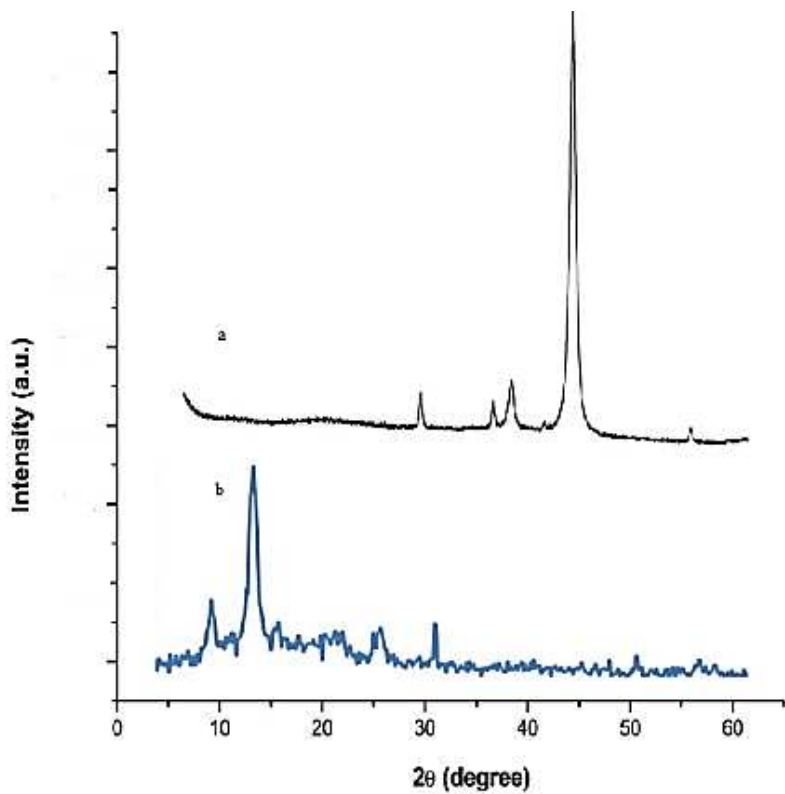


**Figure 8.** XRD pattern for (A) steel samples two hours following immersion in blank solution 0.1M HCl; (B) steel samples two hours following immersion in 100mg/L of Trachyspermum.

XRD pattern illustrated in Figure 8 can obtain the change of mild steel components. As the XRD pattern showed many compounds changed the composition of mild steel after immersion on Trachyspermum solution. Omitting the peak in  $\theta=45^\circ$  can obtain the covering of the metal surface.

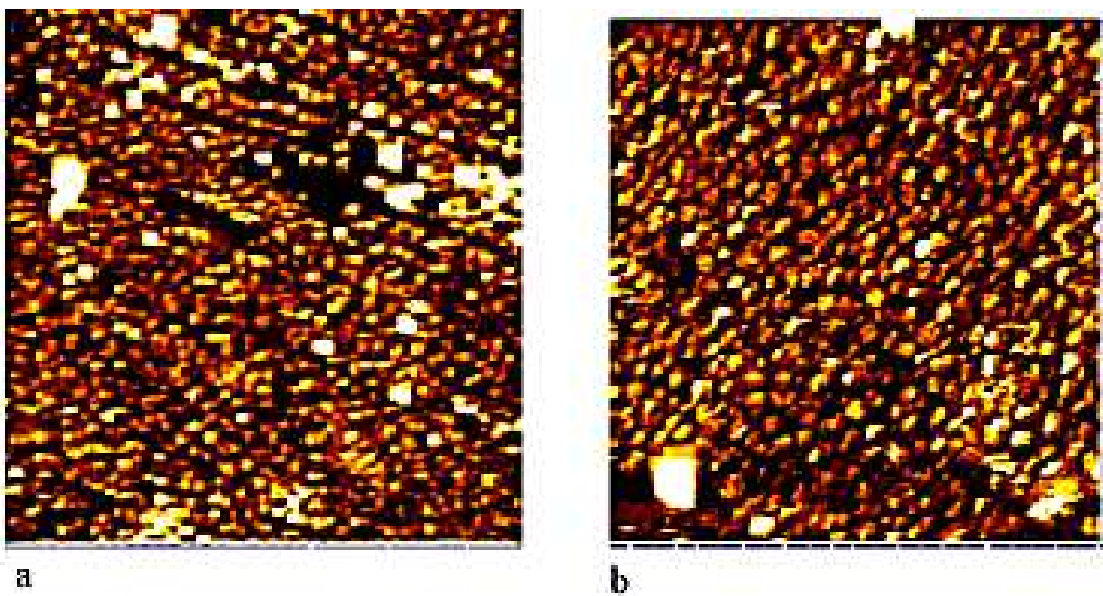


**Figure 9.** AFM images for (A) steel samples two hours following immersion in blank solution 0.1M HCl; (B) steel samples two hours following immersion in 100mg/L of Trachyspermum.

AFM imaging is a method of examining surface roughness. Figure 9 shows the surface of mild steel after 2 hours of immersion in a solution of Trachyspermum extract. As Figure 9 shows, in the absence of Trachyspermum (HCl 0.1M solution), the mild steel surface has many roughnesses and cuts on the surface, which are covered after immersion in the Trachyspermum solution. The compounds in the Trachyspermum extract solution cover the rough surface of the corrosive mild steel. The roughness of the mild steel surface is about 15.2 micrometers before adding Trachyspermum and after adding Trachyspermum changed to  $\approx$ 3 micrometers.

### 3-4. Quantum calculation

Many studies on corrosion inhibitors use quantum chemical estimations of the electronic parameters along with their correlations with the effectiveness of corrosion inhibition calculated through experimental methods. Quantum chemical estimations were performed using the density functional theory (DFT) at a B3LYP function considering 6–311G+ (d, p) basis set for molecules with Gaussian 03 project programming to examine the effects of inhibitor molecular structure as well as electronic features on the effectiveness of inhibition. The optimized structures in the gas phase were considered to obtain the main parameters such as the lowest unoccupied molecular orbital ( $E_{LUMO}$ ) energy, the highest occupied molecular orbital ( $E_{HOMO}$ ), energy gap ( $\Delta E$ ) of the LUMO and HOMO, total energy (T.E.), electronegativity ( $\chi$ ), molecules softness ( $\sigma$ ) as well as hardness ( $\eta$ ), the energy distinction of the molecule electron exchange and dipole moment ( $\mu$ ), chemical potential ( $\pi$ ), the number of transferring electrons ( $\Delta N$ ), etc. the use of the gas phase to perform theoretical estimations is supposed to be a suitable strategy as there are no significant differences with the results of the aqueous phase, while there is a significant decrease in the estimation time. (Tables 4 & 5), including energy gap ( $\Delta E_g$ ), chemical potential ( $\mu$ ), electrophilicity ( $\omega$ ) as well as global hardness ( $\eta$ ) of Trachyspermum (Fig 10) and also the structure of the main materials in Trachyspermum all of which have been considered in research on corrosion inhibition. A critical discussion of the application of this methodology has been provided in another study; it is not possible to provide a straightforward explanation of the corrosion inhibition efficiency just by the use of quantum chemical parameters, reflecting the importance of the nature of the inhibitors effects on the surface. The supporting information represents the estimated electronic parameters along with the relevant discussions on the inhibitors under study. As shown by the specification of the electronic features of isolated

molecules, Trachyspermum can play the most efficient role, supported by the experimental data of this study.

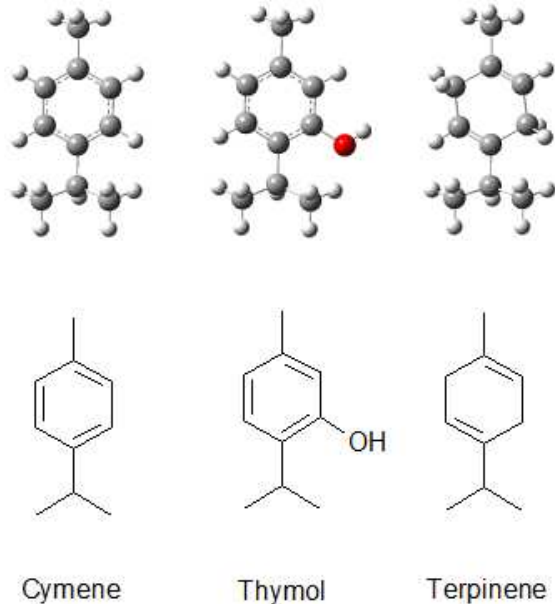


**Figure 10.** Structures of important materials in Trachyspermum.

**Table 4.** Some chemical parameters of materials in Trachyspermum

|                 | Thymol      | Cymene       | Terpinene    |
|-----------------|-------------|--------------|--------------|
| E gas(HF)       | -464.405130 | -389.236252  | -390.300040  |
| E water(HF)     | -464.632904 | -389.4536183 | -390.5514496 |
| $\mu$ gas(D)    | 1.9435      | 0.0461       | 0.0691       |
| $\mu$ water (D) | 2.3923      | 0.0905       | 0.1183       |
| HOMO(HF)        | -0.32265    | -0.34265     | -0.31180     |
| LUMO(HF)        | -0.15828    | -0.16450     | -0.16480     |
| H(HF)           | -464.404186 | -389.224752  | -390.299095  |

|       |             |             |             |
|-------|-------------|-------------|-------------|
| G(HF) | -464.445776 | -389.273613 | -390.341835 |
|-------|-------------|-------------|-------------|

**Table 5.** Molecular electronic parameters(eV) of materials in Trachyspermum

|            | Thymol | Cymene | Terpinene |
|------------|--------|--------|-----------|
| IP         | 8.79   | 9.34   | 8.49      |
| EA         | 4.31   | 4.48   | 4.49      |
| $\chi$     | 6.55   | 6.91   | 6.49      |
| $\mu$      | -6.55  | -6.91  | -6.49     |
| $\sigma$   | 0.45   | 0.41   | 0.5       |
| $\eta$     | 2.24   | 2.43   | 2.00      |
| $\omega$   | 9.57   | 9.82   | 10.53     |
| $\Delta E$ | -4.48  | -4.86  | -4.00     |

### 3-5. Weight loss

The corrosion loss was compared when the inhibitor was absent ( $W_u$ ) and present ( $W_i$ ) to calculate the inhibition degree of surface coverage ( $\theta$ ) at different concentrations of Trachyspermum with the use of the equation below:

$$\eta(\%) = \frac{W_u - W_i}{W_i} \times 100$$

$$\theta = \frac{W_u - W_i}{W_i}$$

The increased efficiency observed for the inhibition based on the concentration can be explained by considering the adsorption scope of the inhibitor molecules on the metal surface. It is supposed that the formation of the film by the inhibitor molecule adsorption on the surface of the metal is the only criterion to lower the surface area of the cathodic and anodic reactions. The inhibitor molecules cover a fraction  $\theta$  of the metal surface at a given instant, while there is a reaction between the uncovered fraction ( $1-\theta$ ) and the acid when the inhibitor is absent. It is possible to deduce the inhibitor's adsorption features according to the nature of the inhibitor interaction with the corroding surface. The adsorption features can be also explained using the values of the surface coverage (Table 6).

**Table 6.** The surface coverage area of mild steel in 0.1M HCl containing Trachyspermum for 24 hours

| C(mg/L)  | 0      | 30     | 45     | 70     | 100    |
|----------|--------|--------|--------|--------|--------|
| $\theta$ | 0.7750 | 0.8210 | 0.8536 | 0.8625 | 0.8954 |

### 3-6. Adsorption isotherm

In general, it is possible to explain the adsorption behavior of inhibitors using adsorption isotherms, indicating critical information on the interactions between metals and inhibitors<sup>54</sup>. As shown by simplifying assumptions, inhibition effectiveness can be considered proportionate to surface coverage<sup>55</sup>. Examination of Frumkin, Temkin, and Langmuir adsorption isotherms as well as the El-Awady kinetic-thermodynamic model<sup>56</sup> aims at fitting the inhibitors' adsorption. Figure 11 shows the curve with a good fitness to Langmuir adsorption isotherm obtained with the use of the equation below<sup>57</sup>:

$$\frac{C}{\theta} = \frac{1}{k_{ads}} + C$$

In which,  $K_{ads}$ ,  $C$ ,  $\theta$ , indicate the equilibrium constant used in the adsorption process, the inhibitor's molar concentration, and the surface coverage, respectively.

the equation below was used to calculate the adsorption free energy ( $\Delta G^\circ_{ads}$ )<sup>58</sup>:

$$\Delta G^\circ_{ads} = -RT\ln(55.5 K_{ads})$$

In which,  $T$  and  $R$  represent the absolute temperature and universal gas constant (8.314 J mol<sup>-1</sup> K<sup>-1</sup>), respectively, while water's molar concentration is considered to be 55.5. When  $\Delta G^\circ_{ads}$  has a value ranging from -20 to -40 kJmol<sup>-1</sup>, there is evidence of both physical and chemical adsorption types<sup>59</sup>. Table 7 indicates the values of  $\Delta G^\circ_{ads}$ .

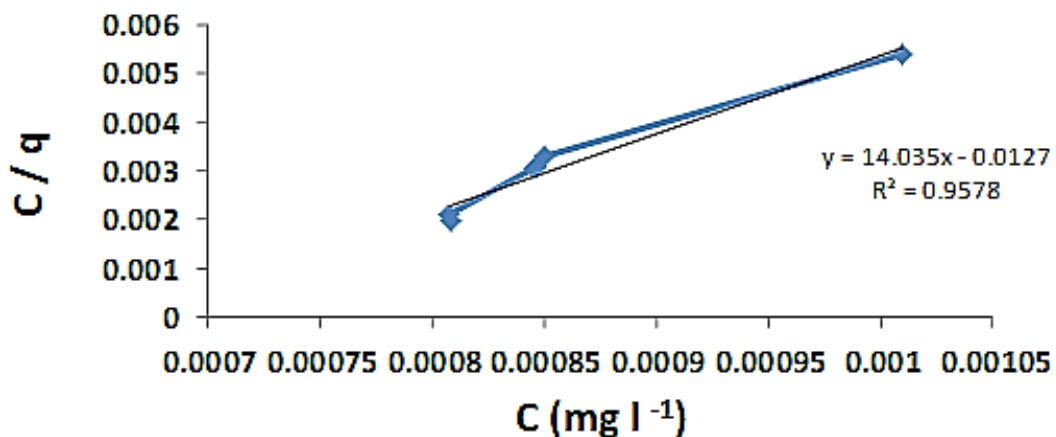


**Figure 11.** Langmuir adsorption plots of Trachyspermum on the steel in 0.1M HCl obtained from results of polarization.

**Table 7.** Results of Langmuir adsorption for investigated inhibitors on the steel in 0.1M HCl obtained from polarization and EIS.

| Inhibitor     | method       | R <sup>2</sup> | K <sub>ads</sub> (M <sup>-1</sup> ) | ΔG° <sub>ads</sub> (kJmol <sup>-1</sup> ) |
|---------------|--------------|----------------|-------------------------------------|-------------------------------------------|
| Trachyspermum | polarization | 0.9578         | 2225                                | -32.2                                     |
| Trachyspermum | EIS.         | 0.9586         | 1851                                | -31.85                                    |

#### 4. Conclusion

Evidence showed that the extract obtained from Trachyspermum had inhibitory effects on mild steel using HCl, while there was an increase in the inhibitory efficacy as the extract concentration increased. The highest value of inhibitory effectiveness was 98% which was obtained at a concentration of 100 ppm. Based on the Potentiodynamic polarization curves, the extract of Trachyspermum leaves could be considered as a mixed inhibitory agent. The adsorption isotherms follow the Langmuir adsorption isotherms. According to the EIS data, the highest coating undamaged index (83 %) after 100 h of immersion. According to the results, the maximum inhibitory effectiveness corresponding to the minimum corrosion rate could be observed at the highest desirable level of inhibitor concentration equal to 100 ppm, while the corrosion rate decreases with an increase in the extract concentration. The absorption examinations indicated the best description of the metal surface interaction by Langmuir isotherm with -31.85Kjmol<sup>-1</sup>, while obtaining the best exposure time for the Trachyspermum leaves extract adsorption into the surface of the metal in different concentrations. SEM, AFM, IR, and XRD showed good coverage of Trachyspermum on the surface of mild steel. Based on the results of polarization, the inhibitors can play the role of a mixed inhibitor, also confirmed by the computational data.

## **Compliance with Ethical Standards**

All of the authors approved that there is no conflict of interest. The authors submitted a statement to the journal office to confirm that the submitted paper is the author's original work. All authors also confirmed that the contents of the submitted paper have not been copyrighted or have not been published previously, it is not being submitted elsewhere, nor it will be published anywhere in any language upon its acceptance.

## **Acknowledgments**

The authors gratefully acknowledge the financial support from the Research Council of Islamic Azad University Kerman branch.

Experimental research and field studies on plants (either cultivated or wild), including the collection of plant material, comply with relevant institutional, national, and international guidelines and legislation.

## **Author Contributions**

N.J. designed the experiments, performed experiments, and collected data; S.A.A. drew all Figures by using Excel software from the data extracted from electrochemical analyzes, discussed the results and strategy, directed and managed the study, and Final approved of the version to be published; R.R. Visualization Critical Revision or Editing of the Article, Final Approval of the Version to be Publish. All authors reviewed the manuscript.

## Data and Software Availability

The datasets generated and/or analyzed during the current study are not publicly available due to ethical reasons but are available from the corresponding author upon reasonable request.

## References

1. Verma, C., Ebenso, E. E., Bahadur, I. & Quraishi, M. A. An overview on plant extracts as environmental sustainable and green corrosion inhibitors for metals and alloys in aggressive corrosive media. *J. Mol. Liq.* **266**, 577–590 (2018).
2. Gao, L., Peng, S., Huang, X. & Gong, Z. A combined experimental and theoretical study of papain as a biological eco-friendly inhibitor for copper corrosion in H<sub>2</sub>SO<sub>4</sub> medium. *Appl. Surf. Sci.* **511**, (2020).
3. Singh, A. *et al.* Comprehensive investigation of steel corrosion inhibition at macro/micro level by ecofriendly green corrosion inhibitor in 15% HCl medium. *J. Colloid Interface Sci.* **560**, 225–236 (2020).
4. Laabaissi, T. *et al.* New quinoxaline derivative as a green corrosion inhibitor for mild steel in mild acidic medium: Electrochemical and theoretical studies. *Int. J. Corros. Scale Inhib.* **8**, 241–256 (2019).
5. Tambun, R., Christamore, E., Pakpahan, Y. F. & Haryanto, B. Banana peel utilization as the green corrosion inhibitor of Iron in NaCl medium. *IOP Conf. Ser. Mater. Sci. Eng.* **420**, (2018).

6. Rouifi, Z. *et al.* Performance and computational studies of new soluble triazole as corrosion inhibitor for carbon steel in HCl. *Chem. Data Collect.* **22**, 100242 (2019).
7. Kamali Ardakani, E., Kowsari, E. & Ehsani, A. Imidazolium-derived polymeric ionic liquid as a green inhibitor for corrosion inhibition of mild steel in 1.0 M HCl: Experimental and computational study. *Colloids Surfaces A Physicochem. Eng. Asp.* **586**, 124195 (2020).
8. Chen, S. *et al.* Camphor leaves extract as a neoteric and environment friendly inhibitor for Q235 steel in HCl medium: Combining experimental and theoretical researches. *J. Mol. Liq.* **312**, (2020).
9. Dehghani, A., Bahlakeh, G., Ramezanzadeh, B. & Ramezanzadeh, M. Integrated modeling and electrochemical study of Myrobalan extract for mild steel corrosion retardation in acidizing media. *J. Mol. Liq.* **298**, (2020).
10. Bouraoui, M. M., Chettouh, S., Chouchane, T. & Khellaf, N. Inhibition Efficiency of Cinnamon Oil as a Green Corrosion Inhibitor. *J. Bio- Triboro-Corrosion* **5**, 1–9 (2019).
11. El Mouaden, K. *et al.* Chitosan polymer as a green corrosion inhibitor for copper in sulfide-containing synthetic seawater. *Int. J. Biol. Macromol.* **119**, 1311–1323 (2018).
12. El Ibrahimy, B. *et al.* Computational study of some triazole derivatives (un- and protonated forms) and their copper complexes in corrosion inhibition process. *J. Mol. Struct.* **1125**, 93–102 (2016).
13. Devikala, S., Kamaraj, P., Arthanareeswari, M. & Pavithra, S. Green Corrosion inhibition of mild steel by asafoetida extract extract in 3.5% NaCl. *Mater. Today Proc.* **14**, 590–601

(2019).

14. Jmiai, A. *et al.* Alginate biopolymer as green corrosion inhibitor for copper in 1 M hydrochloric acid: Experimental and theoretical approaches. *J. Mol. Struct.* **1157**, 408–417 (2018).
15. Bhaskaran, Pancharatna, P. D., Lata, S. & Singh, G. Imidazolium based ionic liquid as an efficient and green corrosion constraint for mild steel at acidic pH levels. *J. Mol. Liq.* **278**, 467–476 (2019).
16. Ikeuba, A. I. & Okafor, P. C. Green corrosion protection for mild steel in acidic media: saponins and crude extracts of *Gongronema latifolium*. *Pigment Resin Technol.* **48**, 57–64 (2019).
17. Saxena, A., Prasad, D., Haldhar, R., Singh, G. & Kumar, A. Use of *Sida cordifolia* extract as green corrosion inhibitor for mild steel in 0.5 M H<sub>2</sub>SO<sub>4</sub>. *J. Environ. Chem. Eng.* **6**, 694–700 (2018).
18. Saxena, A., Prasad, D. & Haldhar, R. Use of *Asparagus racemosus* extract as green corrosion inhibitor for mild steel in 0.5 M H<sub>2</sub>SO<sub>4</sub>. *J. Mater. Sci.* **53**, 8523–8535 (2018).
19. Gupta, N. K., Joshi, P. G., Srivastava, V. & Quraishi, M. A. Chitosan: A macromolecule as green corrosion inhibitor for mild steel in sulfamic acid useful for sugar industry. *Int. J. Biol. Macromol.* **106**, 704–711 (2018).
20. Hassannejad, H. & Nouri, A. Sunflower seed hull extract as a novel green corrosion inhibitor for mild steel in HCl solution. *J. Mol. Liq.* **254**, 377–382 (2018).
21. Desai, P. S. *Azadirachta Indica Leaves Ark's as Green Corrosion Inhibitor for Aluminum*

in HCl Solutions. *Int. J. Emerg. Res. Manag. Technol.* **6**, 159 (2018).

22. Dindodi, N. & Shetty, A. N. Stearate as a green corrosion inhibitor of magnesium alloy ZE41 in sulfate medium. *Arab. J. Chem.* **12**, 1277–1289 (2019).
23. Berrissoul, A. *et al.* a Comparative Study on the Corrosion Behavior of Mild Steel and Aluminum Alloy in Acidic Medium Using Green Corrosion Inhibitor. *E-journal New World Sci. Acad.* **14**, 19–31 (2019).
24. Luo, W. *et al.* A combined experimental and theoretical research of the inhibition property of 2-((6-chloropyridazin-3-yl)thio)-N,N-diethylacetamide as a novel and effective inhibitor for Cu in H<sub>2</sub>SO<sub>4</sub> medium. *J. Mol. Liq.* **314**, (2020).
25. Tabatabaei majd, M., Akbarzadeh, S., Ramezan-zadeh, M., Bahlakeh, G. & Ramezan-zadeh, B. A detailed investigation of the chloride-induced corrosion of mild steel in the presence of combined green organic molecules of Primrose flower and zinc cations. *J. Mol. Liq.* **297**, (2020).
26. Vasyliev, G. & Vorobiova, V. Rape grist extract (*Brassica napus*) as a green corrosion inhibitor for water systems. *Mater. Today Proc.* **6**, 178–186 (2019).
27. Haldhar, R., Prasad, D., Saxena, A. & Kumar, R. Experimental and theoretical studies of *Ficus religiosa* as green corrosion inhibitor for mild steel in 0.5 M H<sub>2</sub>SO<sub>4</sub> solution. *Sustain. Chem. Pharm.* **9**, 95–105 (2018).
28. Naseri, E. *et al.* Inhibitive effect of Clopidogrel as a green corrosion inhibitor for mild steel; statistical modeling and quantum Monte Carlo simulation studies. *J. Mol. Liq.* **269**, 193–202 (2018).

29. Fidrusli, A., Suryanto & Mahmood, M. Ginger extract as green corrosion inhibitor of mild steel in hydrochloric acid solution. *IOP Conf. Ser. Mater. Sci. Eng.* **290**, (2018).
30. El-Sabbah, M. M. B. *et al.* Synergistic Effect between Natural Honey and 0.1 M KI as Green Corrosion Inhibitor for Steel in Acid Medium. *Zeitschrift fur Phys. Chemie* **233**, 627–649 (2019).
31. Cui, G. *et al.* Chitosan oligosaccharide derivatives as green corrosion inhibitors for P110 steel in a carbon-dioxide-saturated chloride solution. *Carbohydr. Polym.* **203**, 386–395 (2019).
32. Zhang, K. *et al.* Amino acids modified konjac glucomannan as green corrosion inhibitors for mild steel in HCl solution. *Carbohydr. Polym.* **181**, 191–199 (2018).
33. Masroor, S. *et al.* Aspartic di-dodecyl ester hydrochloride acid and its ZnO-NPs derivative, as ingenious green corrosion defiance for carbon steel through theoretical and experimental access. *SN Appl. Sci.* **2**, 1–16 (2020).
34. Elabbasy, H. M. & Fouda, A. S. Olive leaf as green corrosion inhibitor for C-steel in Sulfamic acid solution. *Green Chem. Lett. Rev.* **12**, 332–342 (2019).
35. Chen, S., Chen, S., Zhu, B., Huang, C. & Li, W. Magnolia grandiflora leaves extract as a novel environmentally friendly inhibitor for Q235 steel corrosion in 1 M HCl: Combining experimental and theoretical researches. *J. Mol. Liq.* **311**, (2020).
36. Dehghani, A., Bahlakeh, G., Ramezan-zadeh, B. & Ramezan-zadeh, M. Experimental complemented with microscopic (electronic/atomic)-level modeling explorations of Laurus nobilis extract as green inhibitor for carbon steel in acidic solution. *J. Ind. Eng.*

*Chem.* **84**, 52–71 (2020).

37. Tan, B. *et al.* Papaya leaves extract as a novel eco-friendly corrosion inhibitor for Cu in H<sub>2</sub>SO<sub>4</sub> medium. *J. Colloid Interface Sci.* **582**, 918–931 (2021).
38. majd, M. T., Ramezan-zadeh, M., Bahlakeh, G. & Ramezan-zadeh, B. Probing molecular adsorption/interactions and anti-corrosion performance of poppy extract in acidic environments. *J. Mol. Liq.* **304**, (2020).
39. Singh, A. & Quraishi, M. A. Azwain (*Trachyspermum copticum*) seed extract as an efficient corrosion Inhibitor for Aluminium in NaOH solution. *Res. J. Recent Sci.* **1**, 57-61 (2012).
40. Haji Naghi Tehrani, M. E., Ramezan-zadeh, M. & Ramezan-zadeh, B. Highly-effective/durable method of mild-steel corrosion mitigation in the chloride-based solution via fabrication of hybrid metal-organic film (MOF) generated between the active *Trachyspermum Ammi* bio-molecules-divalent zinc cations. *Corros. Sci.* **184**, 109383 (2021).
41. Boujakhrout, A. *et al.* Antioxidant activity and corrosion inhibitive behavior of *Garcinia cola* seeds on mild steel in hydrochloric medium. *J. Mater. Environ. Sci.* **6**, 3655-3666 (2015).
42. Dahmani, M., Et-Touhami, A., Al-Deyab, S. S., Hammouti, B. & Bouyanzer, A. Corrosion Inhibition of C38 Steel in 1 M HCl: A Comparative Study of Black Pepper Extract and Its Isolated Piperine. *Int. J. Electrochem. Sci.* **5**, 1060-1069 (2021).
43. Bouknana, D., Hammouti, B., Messali, M., Aouniti, A. & Sbaa, M. Phenolic and non-

Phenolic Fractions of the Olive Oil Mill Wastewaters as Corrosion Inhibitor for Steel in HCl medium. *Port. Electrochimica Acta* **32**, 1-19 (2014).

44. Tan, B. et al. Papaya leaves extract as a novel eco-friendly corrosion inhibitor for Cu in H<sub>2</sub>SO<sub>4</sub> medium. *J. Colloid Interface Sci.* **582**, 918–931 (2021).
45. Tan, B. et al. Corrosion inhibition of X65 steel in sulfuric acid by two food flavorants 2-isobutylthiazole and 1-(1,3-Thiazol-2-yl) ethanone as the green environmental corrosion inhibitors: Combination of experimental and theoretical researches. *J. Colloid Interface Sci.* **538**, 519-529 (2019).
46. Zuo, X. et al. Research of *Lilium brownii* leaves extract as a commendable and green inhibitor for X70 steel corrosion in hydrochloric acid. *J. Mol. Liq.* **538**, 114914 (2021).
47. Tan, B. et al. Experimental and theoretical studies on the inhibition properties of three diphenyl disulfide derivatives on copper corrosion in acid medium. *J. Mol. Liq.* **298**, 111975 (2020)
48. Tan, B. et al. Insight into anti-corrosion nature of Betel leaves water extracts as the novel and eco-friendly inhibitors. *J. Colloid Interface Sci.* **585**, 287-301 (2021).
49. Frisch, M. J. *et al.* guassian (2019).
50. Devi, G. N. *et al.* Polyamidoaminoepichlorohydrin resin a novel synthetic anti-corrosive water soluble polymer for mild steel. *Prog. Org. Coatings* **109**, 117–125 (2017).
51. Kowsari, E. *et al.* In situ synthesis, electrochemical and quantum chemical analysis of an amino acid-derived ionic liquid inhibitor for corrosion protection of mild steel in 1M HCl solution. *Corros. Sci.* **112**, 73–85 (2016).

52. Farahati, R. *et al.* Synthesis and potential applications of some thiazoles as corrosion inhibitor of copper in 1 M HCl: Experimental and theoretical studies. *Prog. Org. Coatings* **132**, 417–428 (2019).
53. Mehdipour, M., Naderi, R. & Markhali, B. P. Electrochemical study of effect of the concentration of azole derivatives on corrosion behavior of stainless steel in H<sub>2</sub>SO<sub>4</sub>. *Prog. Org. Coatings* **77**, 1761–1767 (2014).
54. J.O. Bockris, A.K.N. Reddy, 2nd ed., Modern Electrochemistry vol. 2B, Kluwer Academic/Plenum Publishers, New York, 2000.
55. Kokalj, A. & Costa, D. Molecular modeling of corrosion inhibitors. *Encycl. Interfacial Chem. Surf. Sci. Electrochem.* 332–345 (2018) doi:10.1016/B978-0-12-409547-2.13444-4.
56. Fateh, A., Aliofkhazraei, M. & Rezvanian, A. R. Review of corrosive environments for copper and its corrosion inhibitors. *Arab. J. Chem.* **13**, 481–544 (2020).
57. Muralisankar, M., Sreedharan, R., Sujith, S., Bhuvanesh, N. S. P. & Sreekanth, A. N(1)-pentyl isatin-N(4)-methyl-N(4)-phenyl thiosemicarbazone (PITSc) as a corrosion inhibitor on mild steel in HCl. *J. Alloys Compd.* **695**, 171–182 (2017).
58. Singh, A., Ansari, K. R., Quraishi, M. A., Lgaz, H. & Lin, Y. Synthesis and investigation of pyran derivatives as acidizing corrosion inhibitors for N80 steel in hydrochloric acid: Theoretical and experimental approaches. *J. Alloys Compd.* **762**, 347–362 (2018).
59. Guo, Y. *et al.* Corrosion inhibition properties of two imidazolium ionic liquids with hydrophilic tetrafluoroborate and hydrophobic hexafluorophosphate anions in acid

medium. *J. Ind. Eng. Chem.* **56**, 234–247 (2017).